JACS
JOURNAL OF THE AMERICAN CHEMICAL SOCIETY
Article
pubs.acs.org/JACS

# Dual Gold Catalysis: Stepwise Catalyst Transfer via Dinuclear Clusters

Mie Højer Larsen,[*,†,‡,§,∥] K. N. Houk,[†] and A. Stephen K. Hashmi[‡,⊥]

[†]Department of Chemistry and Biochemistry, University of California, Los Angeles, California 90095, United States
[‡]Organisch-Chemisches Institut, Ruprecht-Karls-Universität Heidelberg, Im Neuenheimer Feld 270, D-69120 Heidelberg, Germany
[⊥]Chemistry Department, Faculty of Science, King Abdulaziz University, Jeddah 21589, Saudi Arabia

Supporting Information

**ABSTRACT:** The interest in and use of dual gold catalysts is forever increasing, but little is known of the mechanism for the catalyst transfer and its effect on the continued high turnover frequency. Herein, we present a computational investigation of the mechanism for the final intermolecular catalyst transfer in the synthesis of dibenzopentalene from 1-ethynyl-2-(phenylethynyl)benzene. Three different scenarios have been explored: a single catalyst transfer from the monoaurated product complex, the analogous water mediated single transfer, and a dual catalyst transfer from the diaurated product complex. Transition structures have been found for each step of the three possible pathways, and a stepwise dual catalyst transfer has proven to be the lowest energy pathway. We here describe a three-step transfer of two gold moieties from one dibenzopentalene to one diyne. This process directly gives the $\sigma,\pi$-gold coordinated diyne for the further intramolecular cyclization reaction.

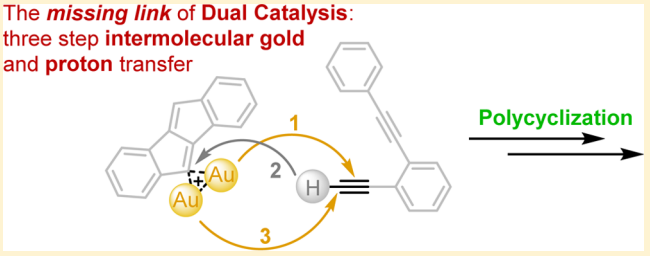


## INTRODUCTION

The active area of gold catalysis has recently focused on dual gold catalysis, the ability of two gold complexes to be involved in one catalytic cycle. For example, gold complexes possessing two gold moieties held together by a linked bisphosphine ligand have enhanced reactivity in oxidative heteroarylations of alkenes[1] and enhanced enantioselectivity in 1,3-dipolar additions.[2] Dimeric gold complexes are also useful as photoredox catalysts for carbon−carbon bond formation.[3] Two gold moieties also can operate through dual catalysis even when not covalently linked. Since its discovery in 2012, many examples of dual gold catalysis of cyclizations of 1,5-diyne to form polycyclic polyaromatic compounds have been reported (Scheme 1).[4] In addition to these cyclizations of 1,5-diynes, a recent study reports the cyclization of the 1,6-diyne product of a Ugi four-component reaction by dual gold catalysis.[5] The mechanistic insights gained from these reactions quickly led to the preparation of a precatalyst, TDAC (*T*raceless *D*ual *A*ctivation *C*atalyst), which delivers the necessary two gold moieties in the needed $\sigma$- and $\pi$-coordinated fashion (Scheme 2).[6] A similar binding picture has been found for both mixed coinage metal $\sigma,\pi$-complexes and for dicopper complexes.[7,8] The former species exhibit interesting luminescence properties, whereas the latter very recently has been identified as key intermediate in the "click reaction".

When TDAC is employed in the cyclization reactions of Scheme 1, the reaction times needed are substantially reduced compared to catalysis by the corresponding single gold catalysts. Further investigation of the reaction course showed that the reduction of the reaction time was due to an almost complete removal of the initiation phase of the reactions.[6] Likewise, a DFT study by Vilhelmsen et al. of the full intramolecular mechanism for the formation of dibenzopentalene **2a** from 1,5-diyne **1a** showed the importance of the dual catalyst.[9] The study showed

**Scheme 1. Cyclization Reactions of 1,5-Diynes**[a]

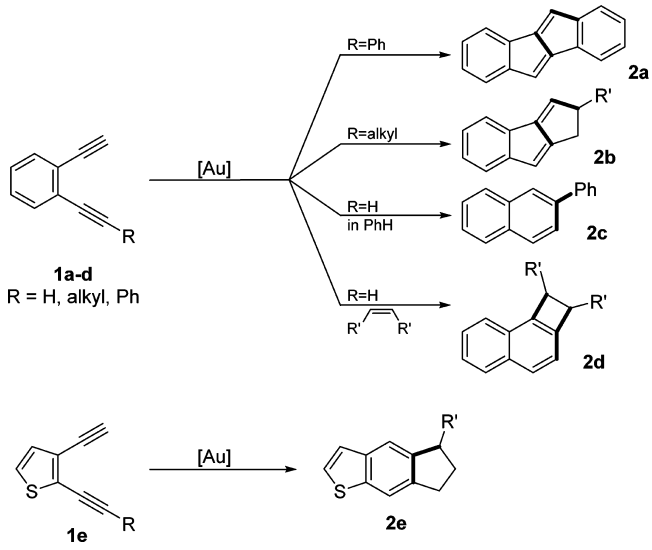


[a]The size of the formed ring (**2a**−**2d** vs **2e**) depends upon the aromatic system present in the diyne **1a**−**1e** and the possible further ring formations upon the substituent R in **1a**−**1d** or the solvent.

**Received:** June 4, 2015
**Published:** August 10, 2015





DOI: 10.1021/jacs.5b05773
J. Am. Chem. Soc. 2015, 137, 10668−10676

**Scheme 2. Dual Activation Catalyst (TDAC) and Its Function in Activation of Diynes Towards Cyclization**[a]

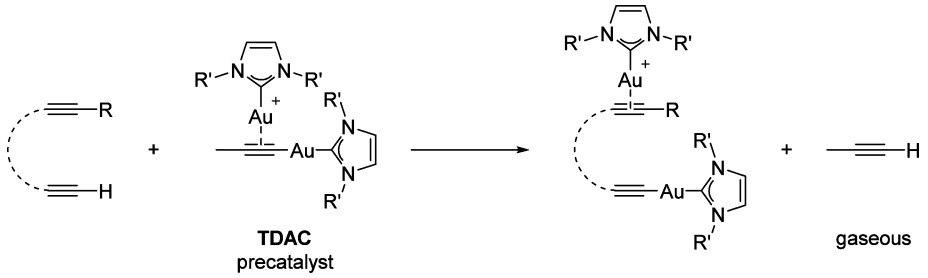


[a]Gaseous propyne is a byproduct.

**Scheme 3. Two Proposed Mechanistic Cycles**[a]

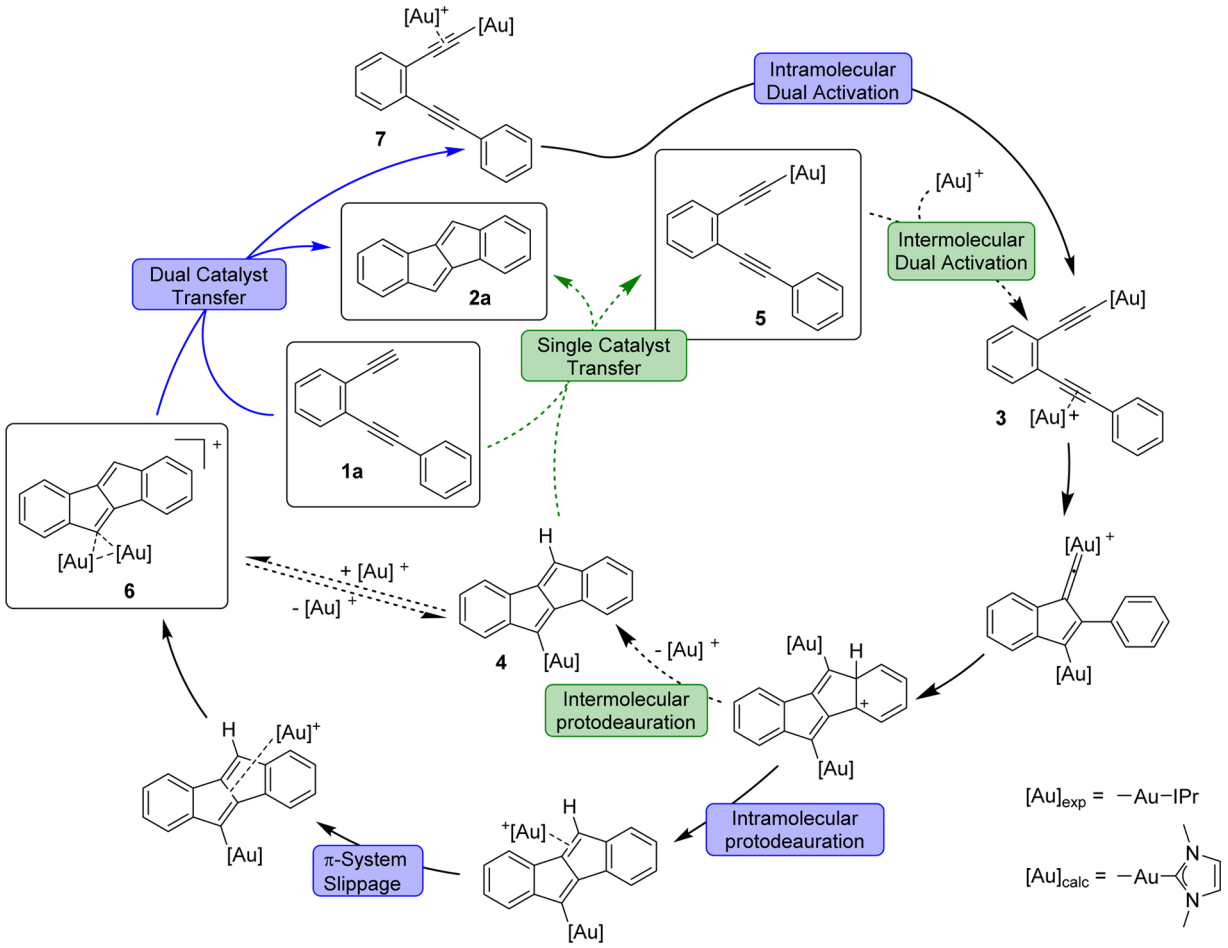


[a]The two gold moieties can either stay as part of the same molecular system and be transferred together (solid arrows) or be transferred individually at different points of the catalytic cycle (dashed arrows). The boxed species have all been isolated and characterized.

that two gold moieties were coordinated to the $\pi$-system at all times (Scheme 3, solid arrows) as opposed to the previously proposed mechanism of two separate replacements of the golds by protodeauration (Scheme 3, dashed arrows). Thermodynamically, the single catalyst transfer was found to be less favorable by 8.4 kcal/mol compared to the dual catalyst transfer. Additionally, whereas the single transfer must be followed by an intermolecular dual activation step by $\pi$-coordination of a second gold moiety, the product of the dual transfer is set up for an immediate intramolecular activation to form complex **3**.

On the basis of these experimental and theoretical findings, we wished to investigate both the originally proposed single catalyst transfer and a dual catalyst transfer and compare the two scenarios. We here show that two golds are needed together not only for the dual activation step, but also to ease the catalyst transfer step, making the overall reaction energetically possible. We now report the *missing link* of the intramolecular mechanism, namely, the catalyst transfer, and show that of the two contemplated scenarios the single catalyst transfer (the step highlighted in green in Scheme 3) is unlikely compared to the dual catalyst transfer (the step highlighted in blue in Scheme 3).



DOI: 10.1021/jacs.5b05773
J. Am. Chem. Soc. 2015, 137, 10668−10676

**Scheme 4. Simultaneous Transfer of the Proton from the Diyne 1a and the Gold Moiety of Dibenzopentalene Complex 4 via Transition State TS1**[a]

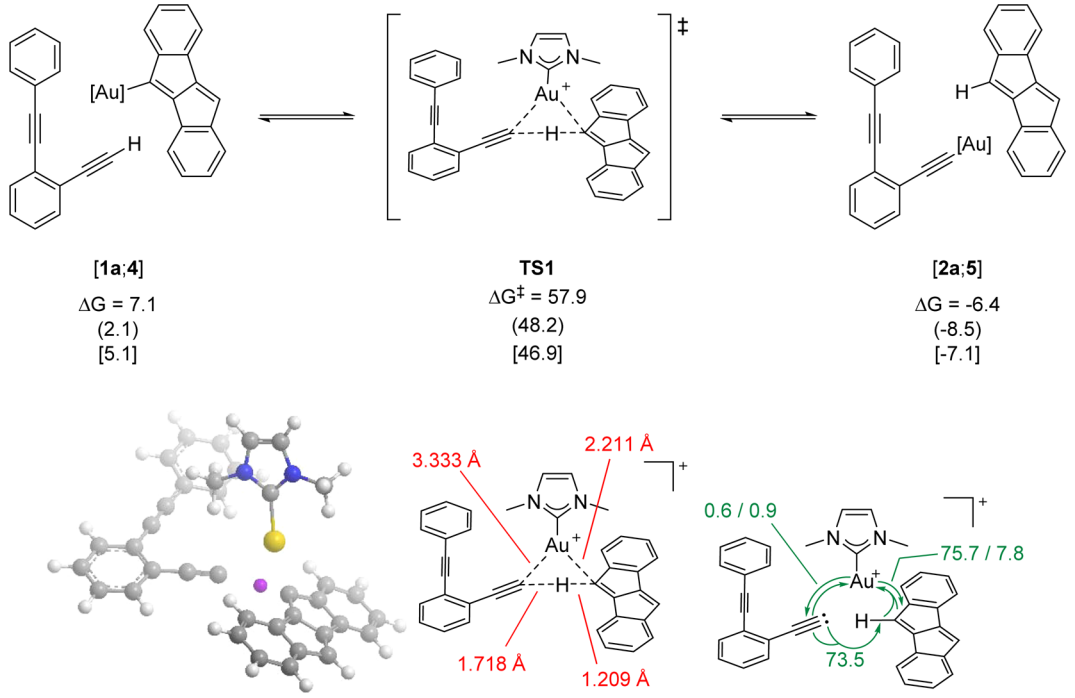


[a]The listed Gibbs free energies are in kcal/mol and are relative to the collected energies of **1a** and **4**; the parenthesized energies are D3 corrected by M06 single point calculations and the bracketed energies are for the solvated species. The DFT optimized transition state structure of **TS1** is shown bottom left. Only the transferring proton is highlighted in purple. Relevant interatom distances are shown in red on the center structure. The NBO representation (bottom left) shows the energy gained by the indicated interactions (in kcal/mol) in green.

## RESULTS AND DISCUSSION

DFT calculations were used to investigate the energetics of the two mechanistic pathways discussed above. The geometry optimizations and transition state searches were performed on the B3LYP level with the cc-pVDZ basis set.[10−12] For gold, additional relativistic effective core potentials were employed.[13,14] Single point calculations were performed at the M06 level with a mixed basis set of SDD for gold[15] and 6-311G(d) for all other atoms. Solvation energy corrections were calculated at the M06 level using the SMD model and with benzene as the solvent. All calculations were performed with the Gaussian 09 program package.[16] Approximate transition structures were located through either a manual or an automatic stepwise decrease of the distance between the transferring atom (hydrogen or gold) and the carbon receiving the moiety in question. After removal of all conformational restrictions, the transition structure was optimized. The calculated reaction profile was verified for each transition state by following the intrinsic reaction coordinate (IRC) toward a set of pre- and post-reaction complexes.[17] These complexes are represented throughout the text as [*X*;*Y*], where *X* and *Y* are the two species constituting the reaction complex. The NBO calculations were performed with the NBO 5.0 program package.[18]

The first reaction step investigated was the single catalyst transfer from the monogold dibenzopentalene complex **4** to the diyne **1a** giving the gold acetylide **5** and the final product **2a** (Scheme 4). The transition state **TS1** for the transfer is very high in energy, and based on both the interatom distances and the NBO analysis, regarding the hydrogen−carbon bond, it seems a late transition state. On the contrary, when examining the position of and the interactions with the gold moiety, the transition state seems to be an early transition state. Both the transferring proton and the gold are closer to the dibenzopentalene unit than they are the diyne. Thus, the NBO analysis shows that a $\sigma$-bond has already formed between the dibenzopentalene and the proton with a bond length of 1.209 Å, whereas the distance to the diyne is 1.718 Å. The former bond length is comparable to the carbon−hydrogen distance in the parent compound (**5**, 1.091 Å). Likewise, the gold moiety is considerably closer to the dibenzopentalene (2.211 vs 3.333 Å), and the NBO analysis shows strong interactions directed from the $\pi$-system toward the gold, but the interactions between the gold and the diyne are negligible. However, when the transition state is subjected to IRC analysis, the process continues smoothly to the product reaction complex [**2a**,**5**].

The high activation barrier calculated for the direct protodeauration of the monocatalyst transfer led to consideration of a water-mediated proton transfer. Experimentally, the reaction is run in nondried benzene in an open system;[4d] thus, there will be a small concentration of water in the reaction mixture.

The transition state discovered in this way, **TS2**, shows water acting as a proton bridge with one hydrogen being accepted from the diyne and one being donated to the dibenzopentalene (Scheme 5). Asynchronous progress of the proton and the gold transfer is observed: the proton-transfer just begins as the gold moiety has completely transferred to the diyne. However, as the hydrogen−carbon bond still has full $\sigma$-character, though elongated, the interaction between the gold moiety and the triple bond is comparable with the $\pi$-coordination seen in complex **8** (C−Au distances: 2.139 and 2.512 Å). The NBO analysis of the transition state shows strong interactions between


DOI: 10.1021/jacs.5b05773
J. Am. Chem. Soc. 2015, 137, 10668−10676

**Scheme 5. Water Mediated Proton Transfer from the Diyne 1a and the Gold Moiety of Dibenzopentalene Complex 4 via Transition State TS2**[a]

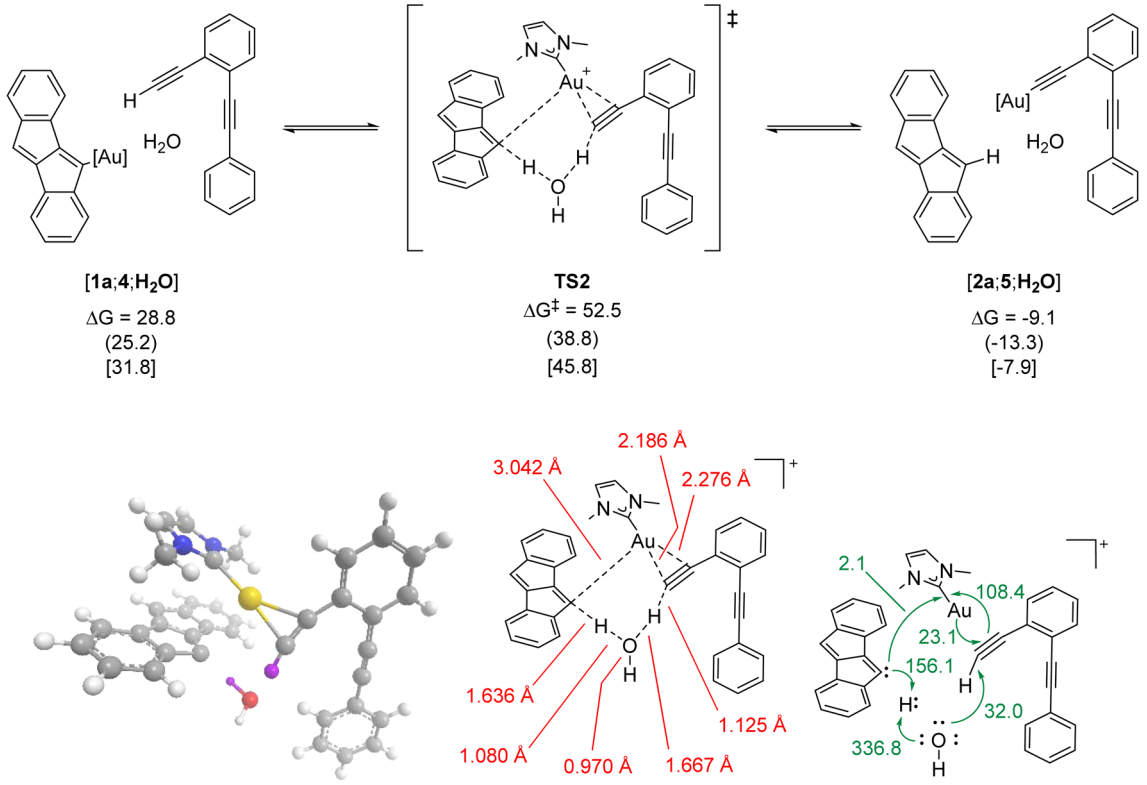


[a]The listed Gibbs free energies are given in kcal/mol and are relative to the collected energies of **1a**, **4** and $H_2O$. The DFT optimized transition state structure of **TS2** is shown bottom left. Only the two transferring protons are highlighted in purple. The NBO representation (bottom left) shows the energy gained by the indicated interactions (in kcal/mol) in green. For further details and color coding, see Scheme 4.

the gold moiety and the diyne triple bond and from both the oxygen of water and the dibenzopentalene toward the transferring proton. As for **TS1**, the interaction between the gold moiety and the secondary carbon species (above the diyne unit, here the dibenzopentalene unit) is almost nonexistent.

The activation energy necessary for the water mediated catalyst transfer and the IRC leading to the reaction complex [**1a**;**4**;$H_2O$] was computed. The activation energy is $\Delta\Delta G^{\ddagger}_{benzene}$ = 14.0 kcal/mol ($\Delta\Delta G^{\ddagger}_{gas}$ = 23.7 kcal/mol). This low barrier starts from complex and does not take into account that water-mediated transfer requires three species to come together. Calculating the activation energy from the separate species (**1a**, **4**, and water) shows that the transfer requires an activation energy comparable to the nonwater mediated reaction, namely, $\Delta G^{\ddagger}_{benzene}$ = 45.8 kcal/mol ($\Delta G^{\ddagger}_{gas}$ = 52.5 kcal/mol) compared to $\Delta G^{\ddagger}_{benzene}$ = 46.9 kcal/mol ($\Delta G^{\ddagger}_{gas}$ = 57.9 kcal/mol) for the transfer under "dry" conditions (Figure 1). The water mediated catalyst transfer was therefore rejected for being as unlikely as the originally proposed single catalyst transfer. However, a recent comparison of thermodynamic and kinetic experiments with theoretical results by Singleton calls for caution when considering explicit solvent mediation purely by theoretical means.[19] They found great differences between the theoretically predicted mechanism involving proton-shuttle processes and the experimentally determined mechanism and energetics of a simple two-step acid–base reaction with the solvent, methanol. Thus, the presence of an acid or base catalyst, even adventitious, might make the water mediated process more favorable. Previously published experimental results on the cyclization of terminally deuterium labeled dialkyne **1a** show some loss of the deuterium upon cyclization (~40% incorporation),[4d] likely due to the presence of some water in the solvent, giving credence to the cautioning from Singleton. However, experiments on the analogous naphthalene synthesis (**2c**, Scheme 1) with the unlabeled dialkynes and an excess addition of $D_2O$ showed only 31% incorporation of deuterium in the final product. This led to the conclusion that the protons of the product originate from the alkyne itself and that a presence of water in the solvent can only be ascribed a minor role.[4b]

The method described above for locating the transition states by stepwise decrease of atom distances led to a revision of the originally sketched pathways of the dual catalyst transfer from the diaurated dibenzopentalene **6** to the diaurated diyne **7**. The dual transfer was thought to proceed by a transfer of one gold to form the $\pi$-complexed diyne **8** followed by a protodeauration or reversed: a protodeauration of one gold moiety from the dibenzopentalene to the diyne followed by a transfer of the now $\pi$-coordinating gold moiety of **9** (Scheme 6, panels a and b, respectively). However, the discovered reaction path is a three-step transfer, highlighted in black in Scheme 6. Furthermore, in case of the dual catalyst transfer, several intermolecular approaches are possible. These were examined, and a perpendicular, sideways approach of the diyne was found to be slightly lower in energy compared to an approach in which the diyne moves between the two gold moieties of **6** prior to the first gold transfer. Finally, for the initial gold transfer, there is the possibility of an intramolecular shift of the gold species to the internal triple bond or that the transfer occurs directly to this


DOI: 10.1021/jacs.5b05773
J. Am. Chem. Soc. 2015, 137, 10668–10676

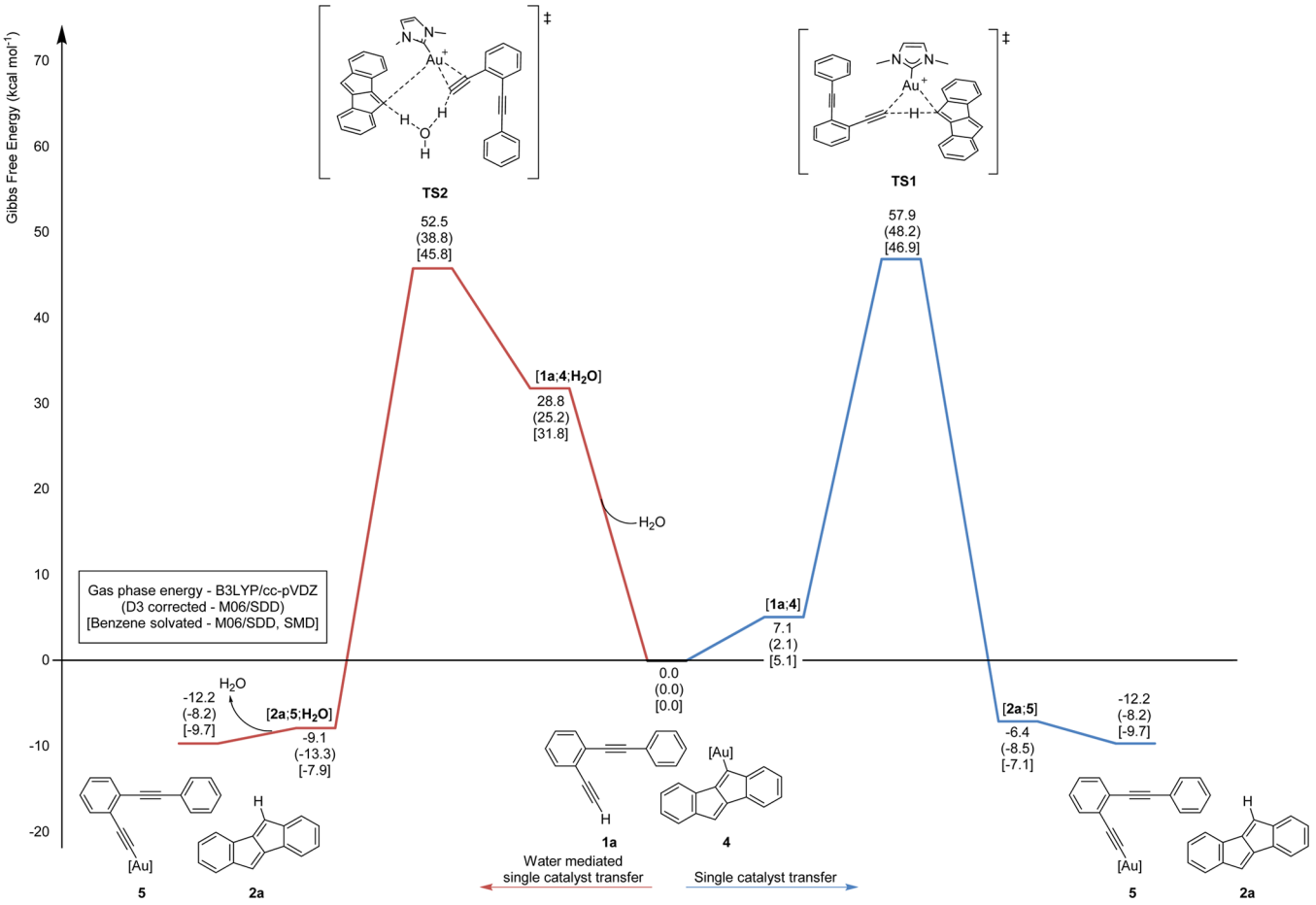


**Figure 1.** Full energy profile of the single catalyst transfer processes either water mediated (in red) or neat (in blue), the energy profile is shown for the energies obtained for the benzene solvated species.

**Scheme 6. Two Proposed Paths for the Dual Catalyst Transfer (a and b) and the Reaction Path Actually Found (Highlighted in Black)**[a]

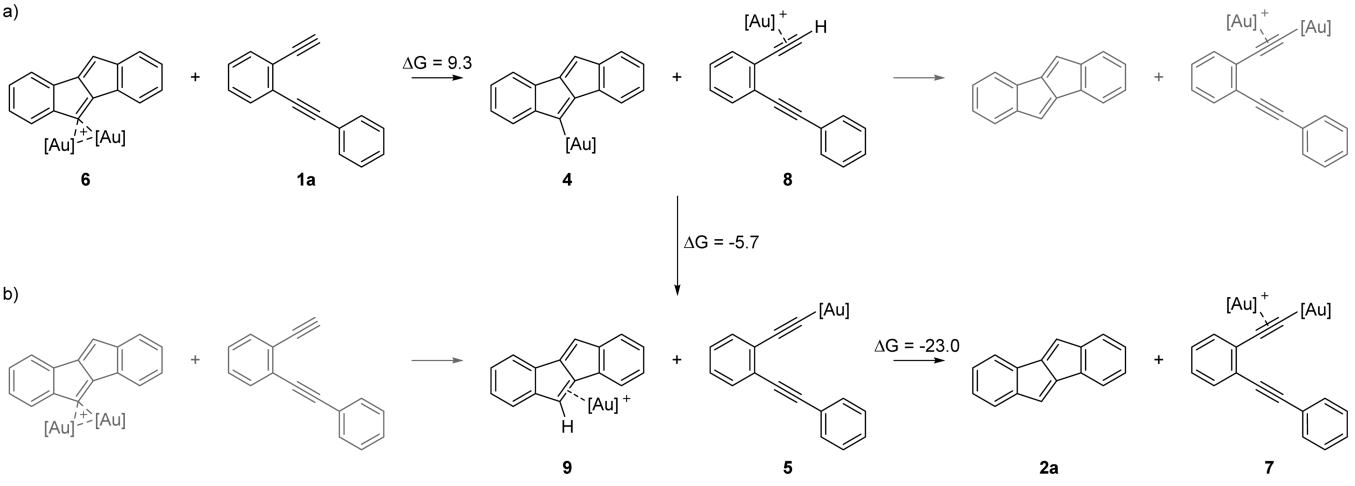


[a]Energies are given in kcal/mol and are calculated from the energies of the separate species in the gas phase.

internal triple bond (structure **S1**). However, thermodynamically, this complex is higher in energy ($\Delta G_{gas}$ = 4.4 kcal/mol) than complex **8**, and thus, the equilibrium between the two $\pi$-complexes is in favor of coordinating the gold at the terminal alkyne. Likewise, previous results show a clear preference for the formation of the diaurated acetylide compared to $\pi$-coordination of the second gold moiety either to the central benzene ring of the diyne ($\Delta G_{gas}$ = 16.5 kcal/mol) or even to the benzene solvent ($\Delta G_{gas}$ = 29.0 kcal/mol).[9]

Each transition state is connected to a pre- and a post-reaction complex; IRC calculations show that there are two different conformations and energies for the reaction complexes [**4**;**8**] and


DOI: 10.1021/jacs.5b05773
J. Am. Chem. Soc. 2015, 137, 10668−10676

**Scheme 7. Transfer of the NHC-Au$^+$ Moiety, Giving the $\pi$-Coordinated Diyne Complex 8 via Transition State TS3**[a]

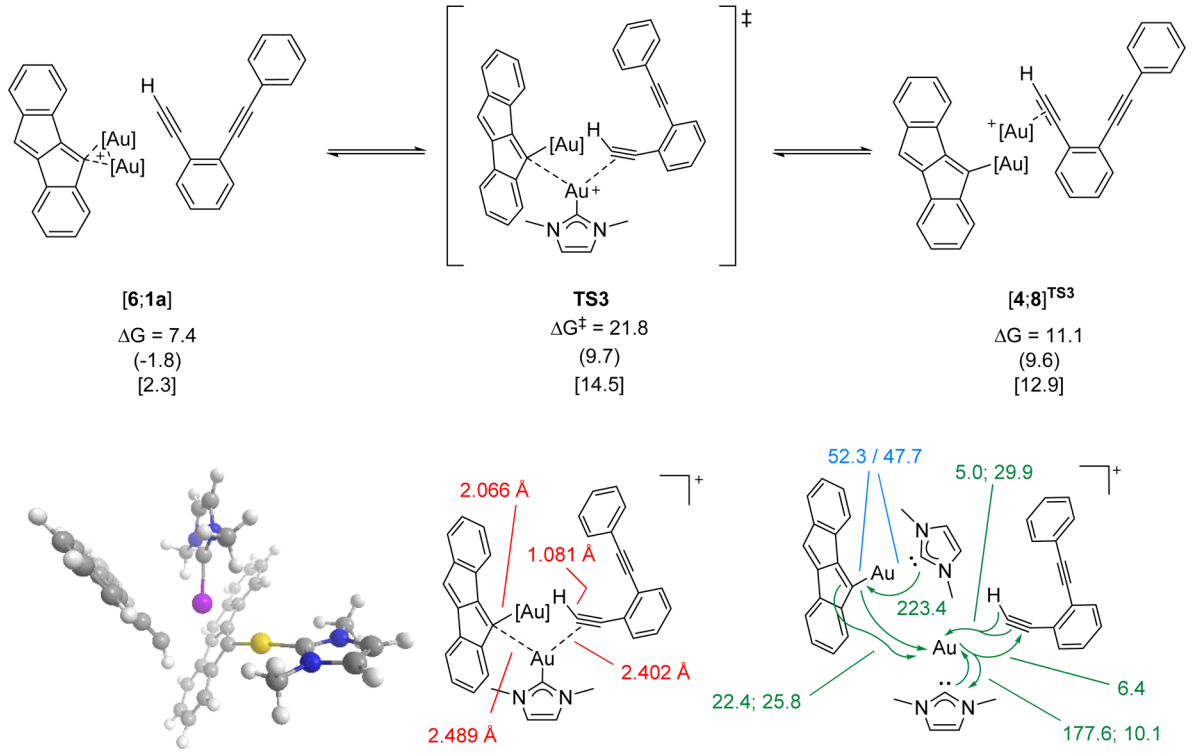


[a]The listed Gibbs free energies are given in kcal/mol and are relative to the collected energies of **1a** and **6**. The DFT optimized transition state structure of **TS3** is shown bottom left. The gold of the transferring catalytic moiety is highlighted in purple. The numbers in blue on the NBO representation (bottom left) give the hyperbond distribution for the indicated bonds (in percent) and the energy gained by the indicated interactions (in kcal/mol) in green. For further details and color coding, see Scheme 4.

**Scheme 8. Transfer of the Proton via Transition State TS4 To Form the $\pi$-Complexed Dibenzopentalene 9**[a]

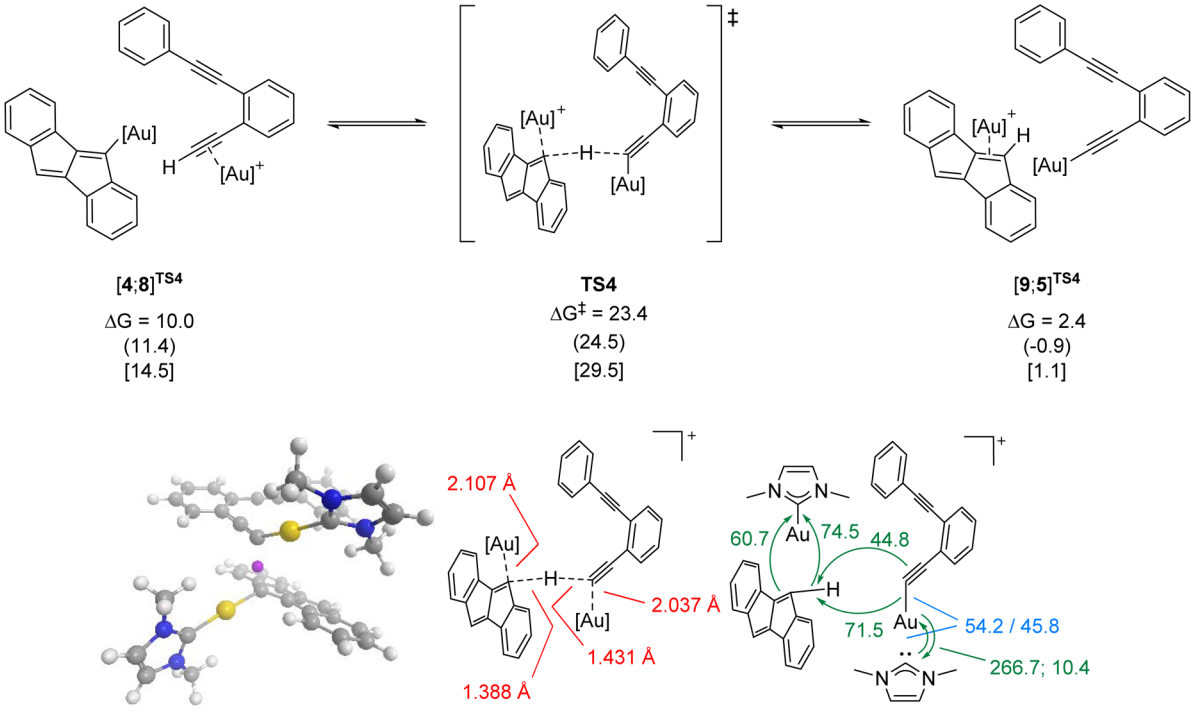


[a]The listed Gibbs free energies are given in kcal/mol and are relative to the collected energies of **1a** and **6**. The DFT optimized transition state structure of **TS4** is shown bottom left. The transferring proton is highlighted in purple. The numbers in blue on the NBO representation (bottom left) give the hyperbond distribution for the indicated bonds (in percent). For further details, color coding and units see Scheme 4.



DOI: 10.1021/jacs.5b05773
J. Am. Chem. Soc. 2015, 137, 10668−10676

**Scheme 9. Transfer of the Gold Moiety via Transition State TS5 To Form the Diaurated Diyne 7**[a]

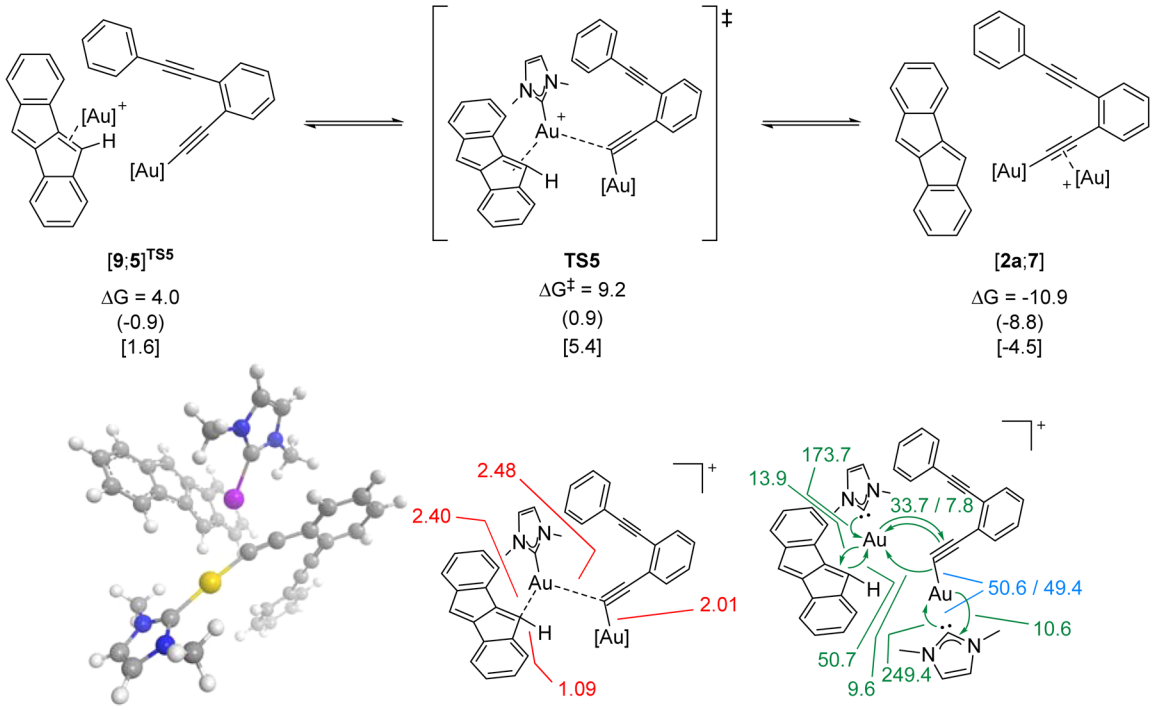


[a]The listed Gibbs free energies are given in kcal/mol and are relative to the collected energies of **1a** and **6**. The DFT optimized transition state structure of **TS5** is shown bottom left. The transferring gold moiety is highlighted in purple. The numbers in blue on the NBO representation (bottom left) give the hyperbond distribution for the indicated bonds (in percent) and the energy gained by the indicated interactions (in kcal/mol) in green. For further details and color coding, see Scheme 4.

[**5**;**9**]. They will be distinguished by their attachment to either of the transition states **TS3**, **TS4**, and **TS5**.

The initial step of the dual catalyst transfer can effectively be seen as an intermolecular $\pi$-system slippage. One gold moiety of the diaurated dibenzopentalene becomes $\pi$-coordinated to the terminal acetylene of the diyne, while the other shifts and becomes fully $\sigma$-bonded to the dibenzopentalene. In the transition state, the transferring gold moiety is placed further from the dibenzopentalene than from the diyne (see Scheme 7). However, examination of the transition state by NBO analysis showed that the strongest interactions are the ones between the gold moiety and the dibenzopentalene system. The carbon−gold bond length for the remaining gold moiety to the dibenzopentalene unit in **TS3** (2.066 Å) is slightly longer than for the corresponding monoaurated species **4** (2.035 Å), but shorter than the bond length in the diaurated complex **6** (2.150 Å). The bond length of the carbon−hydrogen bond in **TS3** (1.081 Å) emphasizes the $\pi$-complex character of the gold−acetylene interaction. The bond length is comparable to the bond length found in the gold $\pi$-complex **8** (1.084 Å) rather than the shorter bond found in the parent diyne **1a** (1.072 Å). Finally, the short distance (2.86 Å) between the two gold atoms in the diaurated complex **6**, and the resulting aurophilic interactions are somewhat preserved in the transition state before being broken in complex [**4**;**8**]$^{TS3}$. Thus, the distance between the two gold atoms are 3.01 Å in **TS3**, and the NBO analysis shows a slight interaction directly between the two gold atoms of 7.4 kcal/mol.

The next step of the dual catalyst transfer is the transfer of the proton from the diyne via the transition state **TS4** (Scheme 8). This necessitates that the two gold moieties shift from being $\sigma$-bonded to $\pi$-complexes in the dibenzopentalene unit **9** and vice versa for the diyne complex **8**. The change in the bonding character for all three species is apparent when analyzing the transition state in terms of bond lengths and NBOs (Scheme 8, bottom). The transition state appears to be a late transition state, as the NBO bond analysis shows that $\sigma$-bonds have developed between the proton and the dibenzopentalene unit and between one of the gold moieties and the diyne. Conversely, the bond between the second gold and the dibenzopentalene has weakened, and the gold moiety is held by interactions with the $\pi$-system and the newly formed carbon−hydrogen bond. However, the interatom distance between the gold and the dibenzopentalene (2.107 Å) strongly resembles the distance found in the diaurated complex **6**, where the bonding character toward each gold atom is $\sigma$-like. The $\sigma$-character of the carbon−gold bond between gold moiety previously complexed to the $\pi$-system of the diyne and the terminal carbon of the diyne is emphasized by the bond length between the two (2.037 Å). The bond length is intermediate between the bond length found in **5** and **8** (1.984 and 2.139 Å, respectively). The interatom distances between the carbons of the diyne and the dibenzopentalene and the transferring proton (1.431 and 1.388 Å, respective) are both greater than the carbon−hydrogen bond lengths in either of the parent complexes **1a** and **2a**. In accord with the interactions found by NBO analysis, the distance between the dibenzopentalene carbon and the hydrogen is slightly shorter than the distance toward the diyne.

Finally, the second gold is transferred, once again from one $\pi$-system to the other (Scheme 9). The transition step **TS5** shows a gold moiety midway in the transfer and both the bond lengths, and the NBO analysis of the transition state shows an almost equal affiliation with both carbon systems. The gold−carbon distances toward both the diyne and the dibenzopentalene units (2.48 and 2.40 Å, respectively) are slightly longer than the parent


DOI: 10.1021/jacs.5b05773
J. Am. Chem. Soc. 2015, 137, 10668−10676

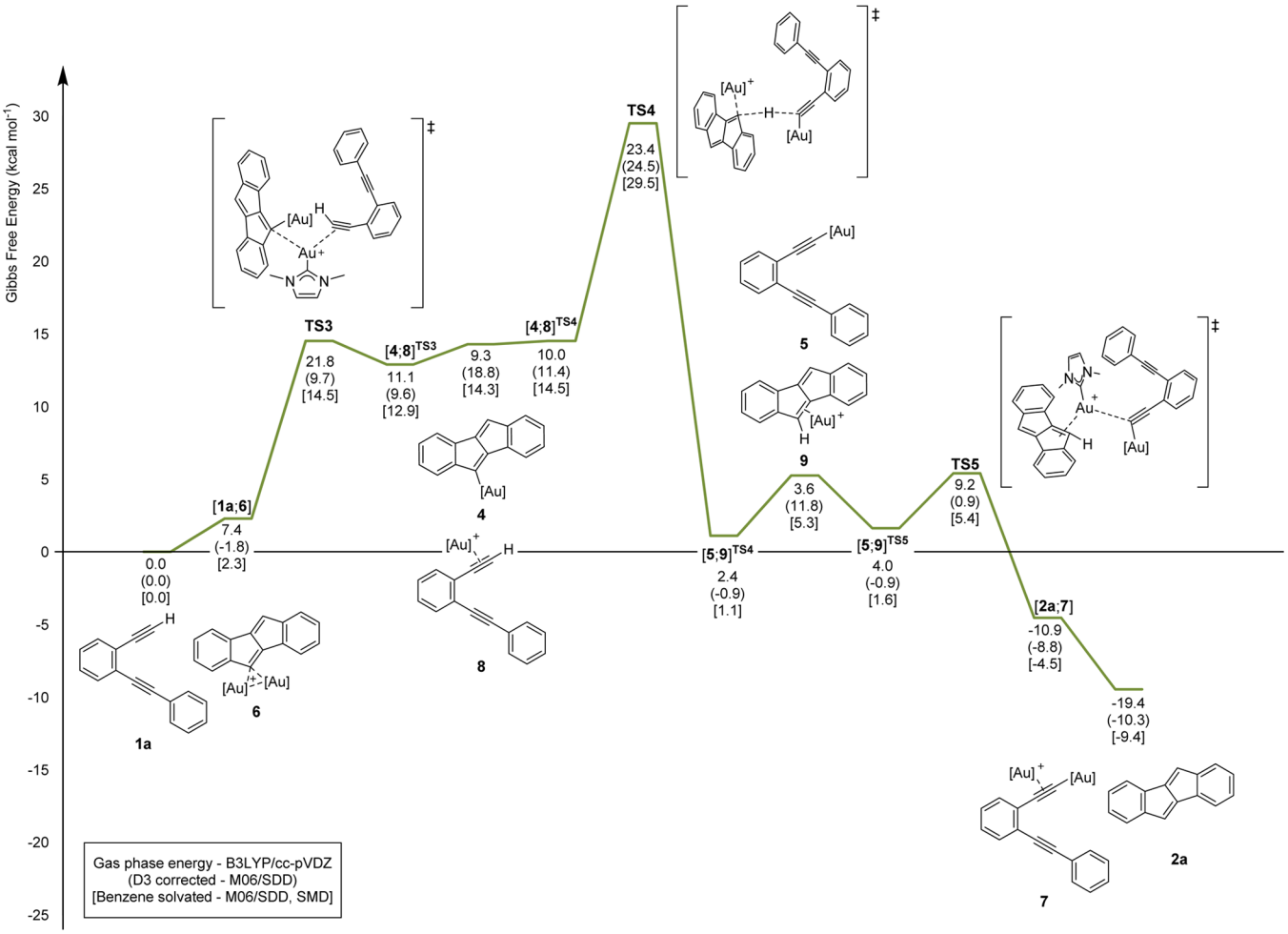


**Figure 2.** Full energy profile of the dual catalyst transfer process, the energy profile is shown for the energies obtained for the benzene solvated species.

diaurated diyne **7** and the $\pi$-complex **9** (2.14 and 2.30 Å, respectively). Neither the carbon−hydrogen bond length in the dibenzopentalene fragment nor the gold−carbon bond length in the diyne fragment is affected by the transferring gold moiety when compared to the corresponding $\sigma$-bonds in complexes **2a** and **7**. Finally, in **TS5**, the two gold moieties are now within short enough distance (3.83 Å) to once again establish a minor aurophilic interaction. NBO analysis predicts the interaction to be of 1.1 kcal/mol in strength.

Figure 2 shows the full energy profile of the dual catalyst transfer. The overall activation energy for the dual process is 29.5 kcal/mol in benzene (23.4 kcal/mol in the gas phase), corresponding to the energy level of **TS4**, the proton transfer. Despite this relatively high activation barrier, it should be noted that the overall reaction is exothermic by 9.4 kcal/mol in benzene (and 19.4 kcal/mol in the gas phase) and that this will drive the catalyst transfer toward the dual activated diyne **7**. In comparison, the activation energy required for the mono transfer is considerably higher, while the thermodynamic gain of the catalyst transfer is unchanged ($\Delta G_{benzene}$ = −9.7 kcal/mol).

## CONCLUSION

Computational studies have closed the mechanistic cycle for the dual gold catalyzed formation of dibenzopentalene **2a** from 1,5-diyne **1a** and showed that there is a significant energetic gain in keeping the two gold moieties together throughout the reaction. The activation energies in benzene for the three processes examined here—the single catalyst transfer, the water mediated single catalyst transfer, and the dual catalyst transfer—were determined to be 46.9, 45.8, and 29.5 kcal/mol, respectively. The high energy requirements of the single catalyst transfers makes the route unlikely compared to the dual transfer. The dual catalyst transfer was found to proceed in three steps: (1) transfer of one gold moiety to form $\pi$-complex **8**, (2) proton transfer, and (3) a second gold transfer of the $\pi$-complexed gold moiety of complex **9**. The calculated overall activation energy of the catalyst transfer ($\Delta G^{\ddagger}_{benzene}$ = 29.5 kcal/mol; $\Delta G^{\ddagger}_{gas}$ = 23.4 kcal/mol) is slightly higher than the previously reported activation energy for the intramolecular steps of the cyclization process ($\Delta G^{\ddagger}_{gas}$ = 18.9 kcal/mol).[9] However, reaching the starting point for the dual catalyst transfer, the diaurated dibenzopentalene **6**, by the intramolecular cyclization, has previously been calculated to be exothermic by 35.8 kcal/mol. Thus, the activation energy found for the intermolecular dual catalyst transfer does not change the overall energy requirements for the cyclization reaction.

## ASSOCIATED CONTENT

### Supporting Information

The Supporting Information is available free of charge on the ACS Publications website at DOI: 10.1021/jacs.5b05773.

Full computational details including all references, structures, and full Z-matrix for all calculated species (PDF)



DOI: 10.1021/jacs.5b05773
J. Am. Chem. Soc. 2015, 137, 10668−10676

## AUTHOR INFORMATION


### Corresponding Author

*E-mail: mhv@oci.uni-heidelberg.de

### Present Address

[‖]University of Copenhagen, Department of Chemistry, Universitetsparken 5, DK-2100 Copenhagen Ø, Denmark.


### Notes

The authors declare no competing financial interest.

[§]Mie Højer Larsen, formally Mie Højer Vilhelmsen.

## ACKNOWLEDGMENTS

We thank the Danish Council for Independent Research | Natural Sciences (M.H.L.) and the National Science Foundation of the U.S.A. (K.N.H., CHE-1361104) for financial support of this research. The authors are thankful for the computational support of the bwGRiD, member of the German D-Grid initiative, funded by the Ministry for Education and Research and the Ministry for Science, Research and Arts Baden-Württemberg.

## REFERENCES


(1) Tkatchouk, E.; Mankad, N. P.; Benitez, D.; Goddard, W. A.; Toste, F. D. *J. Am. Chem. Soc.* **2011**, *133*, 14293−14300.

(2) Martín-Rodríguez, M.; Nájera, C.; Sansano, J. M. *Synlett* **2012**, *2012*, 62−65.

(3) (a) Revol, G.; McCallum, T.; Morin, M.; Gagosz, F.; Barriault, L. *Angew. Chem., Int. Ed.* **2013**, *52*, 13342−13345. (b) McCallum, T.; Slavko, E.; Morin, M.; Barriault, L. *Eur. J. Org. Chem.* **2015**, *2015*, 81−85. (c) Xie, J.; Shi, S.; Zhang, T.; Mehrkens, N.; Rudolph, M.; Hashmi, A. S. K. *Angew. Chem., Int. Ed.* **2015**, *54*, 6046−6050. (d) Kaldas, S. J.; Cannillo, A.; McCallum, T.; Barriault, L. *Org. Lett.* **2015**, *17*, 2864−2866.

(4) (a) Ye, L.; Wang, Y.; Aue, D. H.; Zhang, L. *J. Am. Chem. Soc.* **2012**, *134*, 31−34. (b) Hashmi, A. S. K.; Braun, I.; Rudolph, M.; Rominger, F. *Organometallics* **2012**, *31*, 644−661. (c) Hashmi, A. S. K.; Braun, I.; Nösel, P.; Schädlich, J.; Wieteck, M.; Rudolph, M.; Rominger, F. *Angew. Chem., Int. Ed.* **2012**, *51*, 4456−4460. (d) Hashmi, A. S. K.; Wieteck, M.; Braun, I.; Nösel, P.; Jongbloed, L.; Rudolph, M.; Rominger, F. *Adv. Synth. Catal.* **2012**, *354*, 555−562. (e) Hashmi, A. S. K.; Wieteck, M.; Braun, I.; Rudolph, M.; Rominger, F. *Angew. Chem., Int. Ed.* **2012**, *51*, 10633−10637. (f) Hansmann, M. M.; Rudolph, M.; Rominger, F.; Hashmi, A. S. K. *Angew. Chem., Int. Ed.* **2013**, *52*, 2593−2598. (g) Hansmann, M. M.; Rominger, F.; Hashmi, A. S. K. *Chem. Sci.* **2013**, *4*, 1552−1559. (h) Hansmann, M. M.; Tšupova, S.; Rudolph, M.; Rominger, F.; Hashmi, A. S. K. *Chem. - Eur. J.* **2014**, *20*, 2215−2223. (j) Wieteck, M.; Tokimizu, Y.; Rudolph, M.; Rominger, F.; Ohno, H.; Fujii, N.; Hashmi, A. S. K. *Chem. - Eur. J.* **2014**, *20*, 16331−16336. (i) Tokimizu, Y.; Wieteck, M.; Rudolph, M.; Oishi, S.; Fujii, N.; Hashmi, A. S. K.; Ohno, H. *Org. Lett.* **2015**, *17*, 604−607.

(5) Vachhani, D. D.; Galli, M.; Jacobs, J.; Van Meervelt, L.; Van der Eycken, E. V. *Chem. Commun.* **2013**, *49*, 7171−7173.

(6) Hashmi, A. S. K.; Lauterbach, T.; Nösel, P.; Vilhelmsen, M. H.; Rudolph, M.; Rominger, F. *Chem. - Eur. J.* **2013**, *19*, 1058−1065.

(7) Blanco, M. C.; Cámara, J.; Gimeno, M. C.; Jones, P. G.; Laguna, A.; López-Luzuriaga, J. M.; Olmos, M. E.; Villacampa, M. D. *Organometallics* **2012**, *31*, 2597−2605.

(8) Jin, L.; Tolentino, D. R.; Melaimi, M.; Bertrand, G. *Sci. Adv.* **2015**, *1*, e1500304.

(9) Vilhelmsen, M. H.; Hashmi, A. S. K. *Chem. - Eur. J.* **2014**, *20*, 1901−1908.

(10) (a) Stephens, P. J.; Devlin, J. F.; Chabalowski, C. F.; Frisch, M. J. *J. Phys. Chem.* **1994**, *98*, 11623. (b) Dunning, T. H., Jr. *J. Chem. Phys.* **1989**, *90*, 1007.

(11) For papers on the use of B3LYP for geometry predictions for homogeneous gold catalysis, see: (a) Faza, O. N.; Rodríguez, R. Á.; López, S. C. *Theor. Chem. Acc.* **2011**, *128*, 647−661. (b) Liu, P.; Xu, X.; Dong, X.; Keitz, B. K.; Herbert, M. B.; Grubbs, R. H.; Houk, K. N. *J. Am. Chem. Soc.* **2012**, *134*, 1464−1467. (c) Herbert, M. B.; Lan, Y.; Keitz, B. K.; Liu, P.; Endo, K.; Day, M. W.; Houk, K. N.; Grubbs, R. H. *J. Am. Chem. Soc.* **2012**, *134*, 7861−7866.

(12) For the comparison of fully relativistic methods, see: Pernpointner, M.; Hashmi, A. S. K. *J. Chem. Theory Comput.* **2009**, *5*, 2717−2725.

(13) Peterson, K. A.; Puzzarini, C. *Theor. Chem. Acc.* **2005**, *114*, 283.

(14) Figgen, D.; Rauhut, G.; Dolg, M.; Stoll, H. *Chem. Phys.* **2005**, *311*, 227.

(15) Dolg, M.; Stoll, H.; Preuss, H.; Pitzer, R. M. *J. Phys. Chem.* **1993**, *97*, 5852.

(16) *Gaussian 09*, Revision B.01; Gaussian, Inc.: Wallingford, CT, 2010. See the Supporting Information for the full reference.

(17) (a) Fukui, K. *Acc. Chem. Res.* **1981**, *14*, 363. (b) Gonzalez, C.; Schlegel, H. B. *J. Chem. Phys.* **1989**, *90*, 2154. (c) Gonzalez, C.; Schlegel, H. B. *J. Phys. Chem.* **1990**, *94*, 5523.

(18) *NBO 5.0.*, Theoretical Chemistry Institute, University of Wisconsin, Madison, WI, 2001. See the Supporting Information for the full reference.

(19) Plata, R. E.; Singleton, D. A. *J. Am. Chem. Soc.* **2015**, *137*, 3811−3826.




DOI: 10.1021/jacs.5b05773
*J. Am. Chem. Soc.* 2015, 137, 10668−10676